Shock absorber device on the seismic response of curved viaduct with steel bearing supports

Hokkaido University　Student member　○ Qin TIAN
Hokkaido University　Fellow member　Toshiro HAYASHIKAWA
Hokkaido University　Member　Takashi MATSUMOTO
Hokkaido University　Member　Xingwen HE

1. INTRODUCTION

In earthquake, failure of steel bearings resulted in unseating of decks during the 1995 Kobe earthquake[1)]. Damage of pounding between adjacent viaduct segments, has also been observed in many earthquakes[2)]. To mitigate the above mentioned damage, roller bearings equipped with stopper are installed on the tops of piers. However, pounding force between roller bearing and stopper is so large that can bring damage at not only roller bearing but also the pier bases. So rubber shock absorber device could be used to obviously reduce the pounding force through smooth changes in impact stiffness.

In addition, application of viscous dampers to viaducts has gained significant attention in recent years[3)]. Due to its large resistance force and energy dissipation capacity, viscous dampers have wide application prospect. The most advantage of viscous dampers is that it shows no resistance forces under slow relative movements of segments due to thermal changes, creep and shrinkage effects. It only begins to work when earthquake happens.

Therefore, the purpose of the present study is to analyze the overall performance of highway viaducts with different thickness of rubber shock absorber devices (SADs), considering one kind of viscous damper. The relationship between different thickness of shock absorber device (SAD) and curved viaduct damage can be found. According to the relationship, the advice for the seismic design of curved viaduct based on the appropriate thickness of SAD can be put forward. In addition, a comparison between curved viaducts equipped with SADs and without SADs is also presented.

2. ANALYTICAL MODEL OF VIADUCT

The analytical highway viaduct is composed of a single simply-supported span and a continuous span. The overall viaduct length of 160 m is divided in equal spans of 40 m as shown in **Fig. 1**. The width of superstructure is 11.9 m. The viaduct alignment is horizontally curved in a circular arc with a radius of curvature of 200 m. The curvature is measured from the origin of the circular arc to the centre-line of the deck superstructure. Tangential configuration for both piers and bearing supports is adopted, respect to the global coordinate system for the viaduct as shown in **Fig. 1**, in which the X- and Y- axes lie in the horizontal plane while the Z-axis is vertical. The input ground motion records were measured by the Takatori stations during the 1995 Kobe earthquake. The input ground motion records include three direction earthquake waves which are longitudinal (L), transverse (T) and vertical (V) respectively as shown in **Fig. 2**.

2.1 Superstructure and piers

The viaduct superstructure is composed of a concrete deck slab and three I-section steel girders (G1, G2 and G3). End-span diaphragms and intermediate diaphragms connect the girders together. The distance between adjacent girders in transverse direction is 2.1 m. The space between adjacent diaphragms in tangential direction is 5.0 m. Full composite action between the slab and the girders is simulated by linear elastic elements of the superstructure model, which is represented by the three dimensional grillage beam system as shown in **Fig. 3**. The height of all hollow box section steel piers is 20 m. Flexure fiber element is adopted to represent the

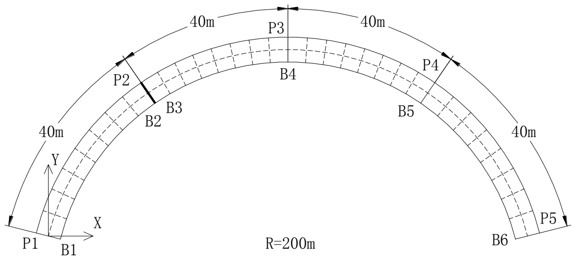

(a) Plan view of curved highway viaduct model

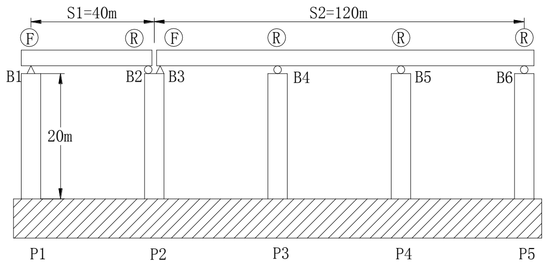

(b) Elevation view of curved highway viaduct model

Fig. 1 Analytical model of viaduct

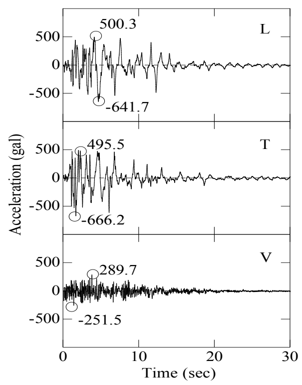

Fig. 2 JR Takatori St. record 1995 Kobe earthquake

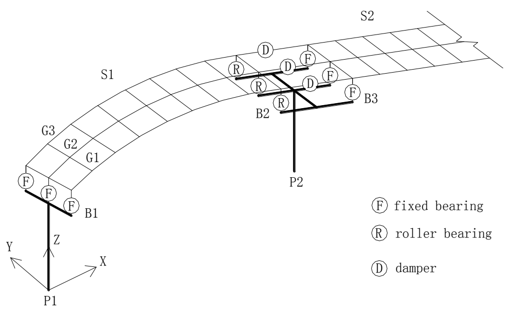

Fig. 3 Curved viaduct finite element model

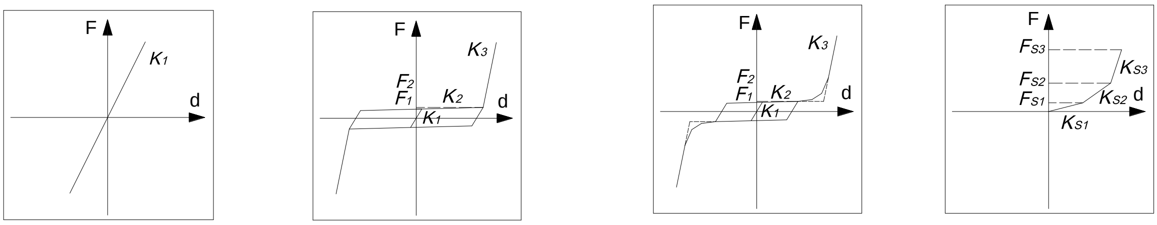

(a) Fixed bearing (b) Roller bearing without SAD (c) Roller bearing with SAD (d) Shock absorber device (SAD)

Fig. 4 Analytical model of steel bearing supports and SAD

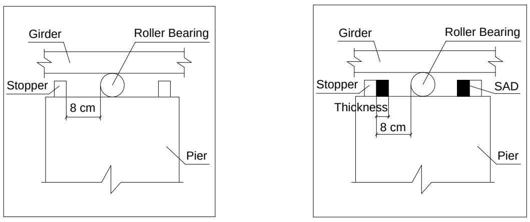

(a) Without SAD (b) With SAD

Fig. 5 Schematic of roller bearing without and with SAD

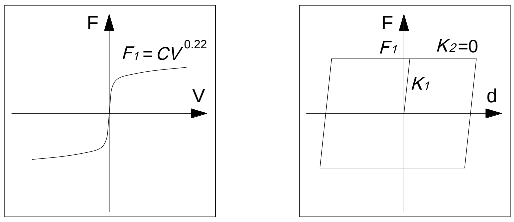

(a) Force-velocity (b) Force-displacement

Fig. 6 Analytical model of viscous damper

Table 1 Cross-sectional properties of deck and piers

Pier or Girder	A (m^2)	I_x (m^4)	I_y (m^4)[a]
P1	0.4500	0.3798	0.3798
P2	0.4700	0.4329	0.4329
P3	0.4700	0.4329	0.4329
P4	0.4700	0.4329	0.4329
P5	0.4500	0.3798	0.3798
G1	0.2100	0.1005	0.0994
G2	0.4200	0.1609	0.2182
G3	0.2100	0.1005	0.0994

[a] I_z in case of G1, G2 and G3.

Table 2 Structural properties of steel bearing supports

Bearing type	Com-ponent	K_1 (MN/m)	K_2 (MN/m)	K_3 (MN/m)	F_1 (MN)	F_2 (MN)
Fixed	Longi-tudinal	980.0	–	–	–	–
	Trans-verse	980.0	–	–	–	–
Roller	Longi-tudinal	49.0	0.0098	980.0	0.0735	0.0743
	Trans-verse	980.0	–	–	–	–

behavior of piers. The cross section of these elements has been divided into a discrete number of longitudinal and transverse fiber regions respectively. The constitutive model of fiber regions is based on uniaxial stress-strain relationship for each zone[4]. The cross-sectional properties of the decks and piers are shown in **Table 1**. In this analysis, steel and concrete densities are 7850 kg/m^3 and 2500 kg/m^3 respectively.

2.2 Bearing supports

For simple supported span, fixed bearing supports (**Fig. 4a**) are installed on the top of left pier (P1), while roller bearing supports are rested on the top of right pier (P2). For continuous span, fixed bearing supports are installed on the top of left pier (P2). However, roller bearings without and with shock absorber device (**Fig. 4b** and **Fig. 4c**) are rested on the top of other piers (P3, P4 and P5). Fixed bearing supports movements are restrained in both longitudinal and transverse radial direction. Roller bearing supports have free movement in longitudinal direction, but have been restrained in transverse radial direction. Structural properties of steel bearing supports are shown in **Table 2**. Schematic of roller bearing without shock absorber device is shown in **Fig. 5a**. Shock absorber device are installed at both sides of all the roller bearings in longitudinal direction as shown in **Fig. 5b**. Based on the previous study, it is obvious that the energy dissipation in SADs is also very small in viaduct system[5]. So, force-displacement relation of shock absorber device could be simulated in **Fig. 4d**. According to previous studies, shock absorber device is effective in reducing negative effects of pounding by smooth changes in impact stiffness. The thickness of SAD is from 0 cm to 8 cm with the increment of 2 cm, in order to keep stiffness as constant value, the section area of SAD is variable. In addition, the stopper gap (8 cm) is adopted in this analysis. Structural properties of SADs are shown in **Table 3**. Therefore, the viaduct seismic performance has been evaluated, based on 5 different thickness of SAD.

2.3 Expansion joint

There is a gap of 10 cm between simply-supported span and continuous span. The gap could become small that leads to pounding phenomenon in earthquakes. The compression-only bilinear gap element is provided with a spring of stiffness 980.0 MN/m that acts when the gap is completely closed. Viscous dampers units are anchored to the three girder ends connecting both adjacent superstructures across the expansion joint. The relationship between resistance force and relative velocity is nonlinear as shown in **Fig. 6a**. C is attenuation coefficient which is shown in **Table 4**. Viscous damper presents no resistance force under slow relative movements of segments resulting from thermal changes, creep and shrinkage effects. It only quickly begins to work when earthquake happens. In other words, viscous dampers do not have influence on viaduct normal service in static state condition that is very well for the viaduct. According to the caculation results, the maximum relative velocity between simple supported span and continuous span is 0.8 m/s while stopper value is 8 cm. The resistance forces of viscous dampers are derived from maximum relative velocity as shown in **Table 4**. Another relationship between force and displacement for viscous damper is shown in **Fig. 6b**. The force-displacement loop is nearly rectangular which presents relative large energy dissipation capacity. In this analysis, viscous damper of KVD500 has been used in the viaduct. Structural properties of viscous damper for KVD500 are shown in **Table 4**.

3. METHOD OF ANALYSIS

The elasto-plastic finite displacement dynamic response analysis is adopted in this analysis. The effects of geometric and material nonlinearities are accounted for through the tangent stiffness matrix. A bilinear type can be used to simulate the stress-strain relationship of beam-column element. The yield stress is 235.4 MPa, the elastic modulus is 200 GPa and the strain hardening in plastic area is 0.01. The kinematic hardening model, unaxial yield criterion flow relations are used to describe the behavior of steel material non-linearity. An incremental-iterative method based on the Newmark direct integration method and the Newton-Raphson iteration scheme is employed for obtaining the solution of the non-linear dynamic equilibrium equations. In addition, a Rayleigh's type has been used to simulate the damping of the structure. Damping coefficient is 2% which is the one of first two natural modes.

4. NUMERICAL RESULTS

4.1 Bearing force

Large pounding force between roller bearing and stopper has negative effect on the bearing damage and piers bases damage. So how to reduce pounding force between roller bearing and stopper is very important. Maximum bearing (B5 and B3) forces are presented in **Fig. 7** and **Fig. 8**, representing maximum roller bearing and maximum fixed bearing forces of continuous span respectively. It can be seen from **Fig. 7** that maximum roller (B5) forces with shock absorber devices are smaller than the case without shock absorber devices. Shock absorber devices can significantly reduce the pounding forces between roller bearing and stopper through smooth changes in impact stiffness. Because the gap value between roller bearing and shock absorber device is less as thickness of shock absorber device is large one, maximum pounding force between roller bearing and stopper decreases with the increase of thickness of shock absorber device. Moreover, **Fig. 7** and **Fig. 8** show that maximum roller bearing (B5) forces are much larger than maximum fixed bearing (B3) forces. In other words, pounding forces between roller bearing and stopper play a more important role in bearing damage and pier base damage than fixed bearing forces.

The pounding force time history between roller bearing (B5) and stopper is analyzed. The force of roller bearing supporting inside girder (G1) and combined with different thickness (T0, T2 and T6) of shock absorber device is presented in **Fig. 9**. Other roller bearing force time history presents the similar change trend. It shows that the application of shock absorber device can obviously reduce roller bearing (B5) forces in both positive and negative directions. Moreover, due to earlier activation of shock absorber device and smooth changes in impact stiffness, contacting time last longer but the pounding forces between roller bearing (B5) and stopper are much

Table 3 Structural properties of shock absorber device

Thickness (cm)	K_{s1} (MN/m)	K_{s2} (MN/m)	K_{s3} (MN/m)	F_{s1} (MN)	F_{s2} (MN)	F_{s3} (MN)
-	-	-	-	-	-	-
2	8.33	100	200	0.10	0.50	1.30
4	8.33	100	200	0.20	1.00	2.60
6	8.33	100	200	0.30	1.50	3.90
8	8.33	100	200	0.40	2.00	5.20

Table 4 Structural properties of viscous dampers

Damper type	Attenuation coefficient C	Power exponent α	Stiffness K_1 (MN/m)	Velocity V (m/s)	Resistance force F_1 (MN)
KVD500	583	0.22	200	0.8	0.555

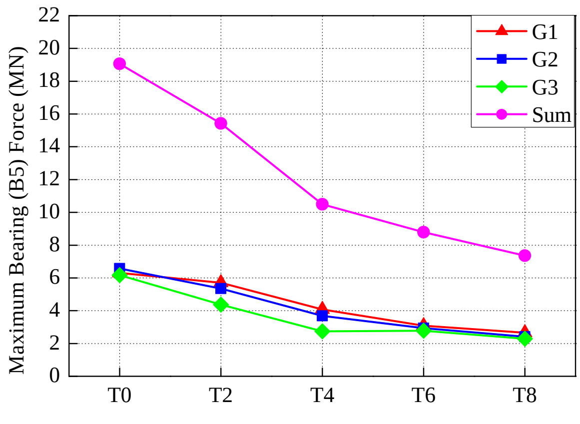

Fig. 7 Maximum roller bearing (B5) forces

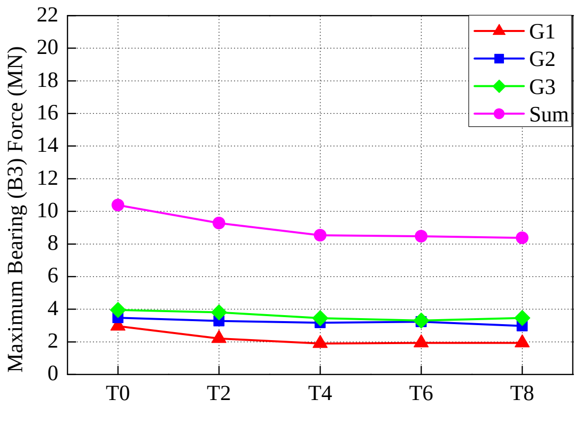

Fig. 8 Maximum fixed bearing (B3) forces

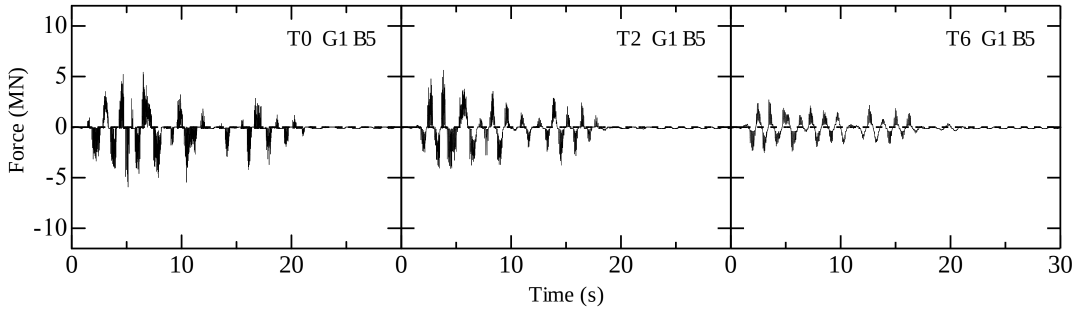

Fig. 9 Roller bearing (B5) force time history

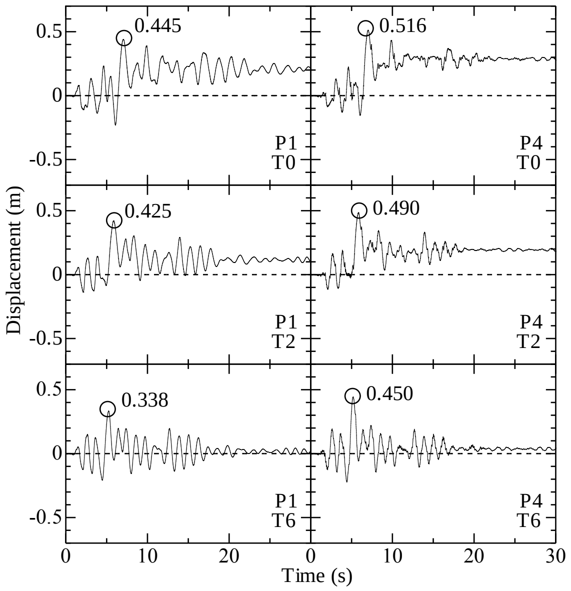

Fig. 10 Displacements time-history on the top of piers (P1 and P4)

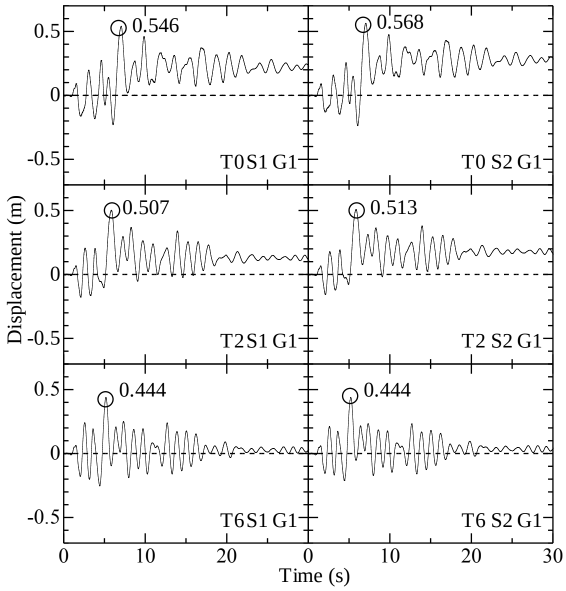

Fig. 11 Displacements time-history of simple supported span (S1) and continuous span (S2)

smaller. As thickness of shock absorber device increases, the pounding forces between roller bearing (B5) and stopper in both positive and negative directions gradually decrease.

4.2 Displacements on the tops of piers

Displacements time-history on the top of piers (in the case of T0, T2 and T6) are shown in **Fig. 10**. Other cases including T4 and T8 present similar change trend. During TAK input earthquakes, displacements on the top of piers present positive direction trend. Viaducts with shock absorber devices present less maximum and less residual displacements in positive direction than those viaducts without shock absorber devices. In addition, maximum and residual displacements in positive direction gradually decrease with the increase of thickness of shock absorber device. Due to both sides of roller bearings equipped with shock absorber devices in longitudinal direction, shock absorber device can reduce maximum roller bearing forces in both positive and negative directions which results in less maximum bending moment and less maximum curvature at piers bases. Consequently, less maximum curvature at piers bases in positive direction results in less maximum and less residual displacements on the top of piers in positive direction as shown in **Fig. 10**. Moreover, pounding forces between roller bearing (supported on the top of P4)　and stopper is obviously larger than fixed bearing (supported on the top of P1) forces. So, maximum and residual displacements on the top of P4 are larger than the one of P1 respectively.

4.3 Displacements of superstructures

Displacements at the right end of simple supported span (S1) and the left end of continuous span (S2) are shown in **Fig. 11**. At the beginning, displacement of simple supported span (S1) and continuous span (S2) presents similarly positive direction trend comparing with displacement on the top of piers. Maximum and residual displacements of superstructures in positive direction could be reduced by shock absorber device. In addition, maximum and residual displacements of superstructures in positive direction decrease with the increase of thickness of shock absorber device. Large thickness of shock absorber device could be activated earlier during earthquakes, which affects on reducing displacements of superstructures in positive direction. In other words, displacements of superstructures are determined by displacements on the top of piers to a certain degree.

5. CONCLUSIONS

The investigation results provide sufficient evidence for the following conclusions:

1) Shock absorber devices could significantly reduce the pounding forces between roller bearing and stopper. As thickness of shock absorber device increases, the pounding forces between roller bearing and stopper obviously decrease. In addition, pounding forces between roller bearing and stopper are much larger than fixed bearing forces. According to roller bearing force time history, in the case of shock absorber devices, contacting time between roller bearing and stopper last longer, but the pounding forces are much smaller.

2) Viaducts with shock absorber devices present less maximum and less residual displacements in positive direction than those viaducts without shock absorber devices. Maximum and residual displacements on the top of piers decrease with the increase of thickness of shock absorber device.

3) Maximum and residual displacements of superstructures present similar change trend with maximum and residual displacement on the top of piers. Maximum and residual displacements on the top of piers play an important role in maximum and residual displacements of superstructures. Moreover, maximum displacement of continuous span (S2) is larger than the one of simple supported span (S1).

REFERENCES

1) Watanabe, E., Sugiura, K., Nagata, K. and Kitane, Y.: “Performances and damages to steel structures during the 1995 Hyogoken-Nanbu earthquake”, Engineering Structures, 20 (4-6), 282-290, 1998.
2) Abdel Raheem, S.E.: Pounding mitigation and unseating prevention at expansion joints of isolated multi-span bridges, Engineering Structures, 31(10): 2345-2356, 2009.
3) Ruangrassamee, A. and Kawashima, K.: Control of nonlinear bridge response with pounding effect by variable dampers, Engineering Structures, 25(5): 593-606, 2003.
4) Mendez Galindo, C., Ruiz Julian, F. D., Hayashikawa, T.: Seismic performance of isolated curved steel viaducts under level II earthquakes, Journal of Structural Engineering, JSCE, 55(A), 699-708, 2009.
5) Kawashima, K. and Shoji, G.: Effect of restrainers to mitigate pounding between adjacent decks subjected to a strong ground motion, 12WCEE, 2000.